

# Urokinase Plasminogen Activator Inhibits HIV Virion Release from Macrophage-Differentiated Chronically Infected Cells via Activation of RhoA and PKC $\epsilon$

Francesca Graziano<sup>1</sup>, Chiara Elia<sup>1</sup>, Carlo Laudanna<sup>3</sup>, Guido Poli<sup>1,2</sup>, Massimo Alfano<sup>1\*</sup>

**1** AIDS Immunopathogenesis Unit, Division of Immunology, Transplantation and Infectious Diseases, San Raffaele Scientific Institute, Milan, Italy, **2** Vita-Salute San Raffaele University, School of Medicine, Milan, Italy, **3** Department of Pathology & Diagnostic, Faculty of Medicine and Surgery, Verona, Italy

## Abstract

**Background:** HIV replication in mononuclear phagocytes is a multi-step process regulated by viral and cellular proteins with the peculiar feature of virion budding and accumulation in intra-cytoplasmic vesicles. Interaction of urokinase-type plasminogen activator (uPA) with its cell surface receptor (uPAR) has been shown to favor virion accumulation in such sub-cellular compartment in primary monocyte-derived macrophages and chronically infected promonocytic U1 cells differentiated into macrophage-like cells by stimulation with phorbol myristate acetate (PMA). By adopting this latter model system, we have here investigated which intracellular signaling pathways were triggered by uPA/uPAR interaction leading the redirection of virion accumulation in intra-cytoplasmic vesicles.

**Results:** uPA induced activation of RhoA, PKC $\delta$  and PKC $\epsilon$  in PMA-differentiated U1 cells. In the same conditions, RhoA, PKC $\delta$  and PKC $\epsilon$  modulated uPA-induced cell adhesion and polarization, whereas only RhoA and PKC $\epsilon$  were also responsible for the redirection of virions in intracellular vesicles. Distribution of G and F actin revealed that uPA reorganized the cytoskeleton in both adherent and polarized cells. The role of G and F actin isoforms was unveiled by the use of cytochalasin D, a cell-permeable fungal toxin that prevents F actin polymerization. Receptor-independent cytoskeleton remodeling by Cytochalasin D resulted in cell adhesion, polarization and intracellular accumulation of HIV virions similar to the effects gained with uPA.

**Conclusions:** These findings illustrate the potential contribution of the uPA/uPAR system in the generation and/or maintenance of intra-cytoplasmic vesicles that actively accumulate virions, thus sustaining the presence of HIV reservoirs of macrophage origin. In addition, our observations also provide evidences that pathways controlling cytoskeleton remodeling and activation of PKC $\epsilon$  bear relevance for the design of new antiviral strategies aimed at interfering with the partitioning of virion budding between intra-cytoplasmic vesicles and plasma membrane in infected human macrophages.

**Citation:** Graziano F, Elia C, Laudanna C, Poli G, Alfano M (2011) Urokinase Plasminogen Activator Inhibits HIV Virion Release from Macrophage-Differentiated Chronically Infected Cells via Activation of RhoA and PKC $\epsilon$ . PLoS ONE 6(8): e23674. doi:10.1371/journal.pone.0023674

**Editor:** Roberto F. Speck, University Hospital Zurich, Switzerland

**Received:** October 29, 2010; **Accepted:** July 25, 2011; **Published:** August 17, 2011

**Copyright:** © 2011 Graziano et al. This is an open-access article distributed under the terms of the Creative Commons Attribution License, which permits unrestricted use, distribution, and reproduction in any medium, provided the original author and source are credited.

**Funding:** This study was supported in part by grants of the VI National Program of Research against HIV/AIDS of the ISS (to MA and GP), by grant of Italian Minister of Health (#40H11 to MA), by the NIH grant n. 1R21 MH075670-01A1 to MA and GP, the Fondation Dormeur to GP, and the Italian Association for Cancer Research (AIRC) 2009–2011, MIUR and Fondazione Cariverona, Verona, Italy, to CL. The funders had no role in study design, data collection and analysis, decision to publish, or preparation of the manuscript. No additional external funding received for this study.

**Competing Interests:** The authors have declared that no competing interests exist.

\* E-mail: massimo.alfano@hsr.it

## Introduction

Urokinase-type plasminogen activator (uPA) is a serine protease that activates plasminogen to plasmin [1] and is synthesized as an inactive precursor (pro-uPA) that undergoes proteolytic activation. Both pro-uPA and uPA bind to a specific glycosyl-phosphatidylinositol (GPI)-anchored receptor, uPAR, on the cell surface [2] and are expressed by inflammatory cells including neutrophils, mononuclear phagocytes (MP), and activated T lymphocytes [2] for which cells they play important roles in cell activation, adhesion and migration. In addition to focusing the proteolytic activity of uPA on the surface of the cells, extracellular uPAR acts as a functional receptor of uPA-dependent signaling [3], inducing cell adhesion, migration, and proliferation in different cell types independently of its catalytic component [4,5].

Of particular relevance is the fact that the uPA system seems to represent an overlapping mechanism involved in both tumor and HIV disease progression [6]. The full-length soluble form of uPAR (suPAR) is predictive of negative clinical outcome in different diseases including cancer [7] and HIV/AIDS. In this latter condition, suPAR represents a novel prognostic indicator which was shown to be independent from and as indicative as low numbers of circulating CD4<sup>+</sup> T cells or high viremia levels [8]. Furthermore, suPAR correlated with the state of immune activation of HIV-infected individuals, as well as with the lipid and glucose metabolism [9]. Of note, higher levels of suPAR were demonstrated not only in the plasma/serum of HIV<sup>+</sup> individuals [10,11], but also in the central spinal fluid (CSF) of neurologically compromised HIV<sup>+</sup> individuals [12,13] and correlated with CSF viral load [13]. Since we have previously reported that uPA

inhibits the release of HIV virions from monocytic cells by inducing their accumulation into intracellular vesicles [14], independently of its enzymatic activity but through binding to uPAR followed by vitronectin dependent adhesion [15] these observations suggest that the increased levels of suPAR may work as a soluble receptor complexing and preventing uPA from exerting an anti-HIV activity *in vivo*.

Since uPAR is GPI-anchored receptor with no intracellular domain it requires the interaction with signaling-competent transmembrane proteins for triggering signal transduction [16]. To date, the most well characterized uPAR partners include integrins [3], the G-protein coupled receptor formyl peptide receptor ligand 1 (FPRL1) [3], and gp130, the signal transducing subunit of the IL-6 R family [17]. uPAR and integrins act as a single functional unit in several cells. Of interest is the fact that monocytes from uPAR-deficient mice fail to adhere onto fibrinogen and to migrate upon thioglycollate stimulation [18] in spite of the expression of the signaling-competent integrin CD11b-CD18 (Mac-1). In this regard, we have recently reported that uPA increased the adhesion to the substrate of both primary human monocyte-derived macrophages (MDM) and of chronically infected promonocytic U1 cells differentiated to macrophage-like cells by phorbol myristate acetate (PMA). Adhesion to the substrate was responsible for uPA-mediated inhibition of HIV expression in these infected cells and was mediated by vitronectin (VN) binding to the uPA/uPAR complex [15]. The ability of the uPA/uPAR/VN complex to redirect virions into intra-cytoplasmic vesicles was independent of the catalytic activity of uPA but was induced by the amino-terminal fragment (ATF) of uPA, competent for intracellular signaling [14,15,19,20]. The general mechanism of uPA-mediated inhibition of HIV replication in macrophages is related to the induction of an increased accumulation of virions budding into intra-cytoplasmic vacuolar compartments of debated nature, a peculiar feature of infected MP not observed in CD4<sup>+</sup> T lymphocytes [21]. This morphological feature of MP has suggested the model of infected macrophages as “Trojan horses” of HIV infection contributing to the generation/maintenance of viral reservoirs in anatomical sites such as the CNS [22]. In addition to other stimuli, including interferon- $\gamma$  (IFN- $\gamma$ ) [23], CCL2 [24], and Mac-1 ligands [14], the uPA/uPAR/VN system might thus represent a mechanism leading to intracellular entrapment of virions into the vesicles.

In this study, we have investigated the nature of the intracellular signaling triggered by uPA/uPAR interaction responsible for the intracellular accumulation of HIV virions. In particular, we have focused our attention on the small GTPase RhoA and PKC isoforms, previously reported to mediate cell motility, chemotaxis, adhesion, migration and stress fiber formation [25], activities that can be mediated by uPA/uPAR interaction independently of uPA catalytic activity [4,5]. In this regard, we have previously demonstrated that uPA induces similar HIV virion morphogenetic features in PMA-differentiated adherent U1 cells [19,26] and in primary MDM either infected *in vitro* [19] or differentiated *ex-vivo* from monocytes of infected individuals [15]. The present study has been performed in the convenient model of PMA-differentiated U1 cells permitting a broader range of experimental conditions than primary MDM obtained from different donors.

## Materials and Methods

### Reagents

LPS-free (bacterial endotoxin  $<2 \times 10^{-5}$  EU/IU corresponding to  $<10^{-10}$  EU/mg) human uPA (M.W. of 52 kDa) was provided by Dr. Jack Henkin (Abbot Laboratories, IL, USA) and Andrew P.

Mazar (Chemistry of Life Processes Institute, Evanston, IL), and was used at 10 nM based on our previous studies [14]. This concentration reflects uPA binding affinity for uPAR (0.1–1 nM) [27] and its levels determined in pathological conditions [28], including serum levels in HIV-1<sup>+</sup> individuals [29]. Hoechst-33342, DNase I Alexa Fluor 488, phalloidin Alexa Fluor 633 were from Molecular Probes (Eugene, OR). Triton X-100, crystal violet, rabbit anti-goat FITC antibodies (Ab) and phorbol-12, myristate-13, acetate (PMA) were purchased from Sigma Chemical Corp. (St. Louis, MO), monoclonal Ab (mAb) against different PKC isoforms were obtained from BD Transduction Laboratories (B-9320 Erembodegem, Belgium), and polyclonal Ab against the phosphorylated form of PKC $\epsilon$  and PKC $\delta$  from Santa Cruz Biotechnology (Santa Cruz, CA). PMA was resuspended in ethanol at 1 mM and used at 10 nM. Cytochalasin D was from Calbiochem (Merck KGaA, Darmstadt, Germany) and was resuspended in DMSO and used at 10  $\mu$ M, based on preliminary experiments identifying non-toxic concentrations for U1 cells, defined as [<sup>3</sup>H]-thymidine uptake and vital cell counts after Trypan blue staining. Penetratin-1 (P1) and P1 fusion peptide containing RhoA/23–40 (P1/23–40), RhoA/92–119 (P1/92–119) and PKC myristoylated pseudosubstrate peptides were dissolved in DMSO at 10 mM and were used at the final concentration of 50  $\mu$ M [30]. Paraformaldehyde (PFA) was purchased from Merck. Round coverslips were from Zeus (Zeus Scientific, Branchburg, NJ), whereas microscope glass slides were obtained from BDH (Poole, UK). Mowiol 4–88 was bought from Calbiochem. Experiments were performed in either standard tissue culture plates (Falcon, BD Biosciences, Bedford, MA) or in Teflon-coated ultra-low adhesion (ULA) plates to rule in/out the contribution of cell adhesion to the investigated hypothesis.

### Chronically HIV-infected U1 cell line

The promonocytic U1 cell line was originally obtained from a population of U937 cells surviving the cytopathic effect of acute CXCR4-dependent HIV-1<sub>LAI/III</sub> infection; each U1 cell contains 2 copies of integrated proviruses [26]. No virus production is detected by conventional reverse transcriptase (RT) activity assay or p24 Gag antigen ELISA in cultures of unstimulated U1 cells, but virus expression at levels comparable to those achieved at peak of acute virus infection of parental U937 cells or primary MDM and T cell blasts is rapidly induced by stimulation of U1 cells with PMA or pro-inflammatory cytokines [26]. U1 cells ( $2 \times 10^5$  cells/ml, unless otherwise indicated, in RPMI 1640 containing 10% of heat-inactivated FCS, 1% pen/strep and 1% glutamine) were incubated with uPA (10 nM), PMA (10 nM) or PMA+uPA in the presence or absence of the above mentioned peptides and reagents. All experiments were performed with U1 cells kept in culture medium containing 10% of FCS because serum starvation (observed at FCS concentrations  $<2\%$ ) prevents uPA-induced adhesion and inhibition of HIV expression, likely consequent to the reduced amounts of VN in the culture medium [15]. Thus, we decide to keep the 10% of serum in our culture medium in order to allow the proper formation of the uPA/uPAR/VN system, and likely the generation of unbiased intracellular signal(s).

### Supernatant- vs. cell-associated virus

HIV-1 virion release in culture supernatants was monitored by determination of Mg<sup>++</sup>-dependent RT activity. Since 99% of the RT enzyme is virion-associated, this assay is a faithful indication of the production of new progeny virions [31]. In order to quantify the levels of cell-associated RT activity, cells were washed twice with culture medium at room temperature and subjected to 5 consecutive cycles of cell freezing and thawing [14].

## U1 cell proliferation and adhesion assay

Cell proliferation and adhesion were measured after 48 h of stimulation in triplicate cultures in 96 flat-bottomed well tissue culture plates, as reported [14,15].

## Optical microscopy

Pictures of cell cultures in the different experimental conditions were acquired with an optical phase contrast Leica DM IL microscope and analyzed by FireCam software (Leica, Deerfield, IL). Pictures of suspended cells or cell clustering were directly taken in the original culture well. Pictures of adherent cells were taken after removal of culture supernatants (i.e., including floating cells, such as present in PMA-stimulated U1 cells, representing about 60% of cells and segregated into the clusters), 2 washes with warm culture medium, 1 wash with 4% PFA in PBS, and 20 min fixation in PFA/PBS at room temperature.

## Quantification of polarized cells

U1 cells were washed and resuspended in culture medium without serum at concentration of  $5 \times 10^5$  cells/ml, and incubated with Cell Tracker Red CMPTX (1  $\mu$ M, Invitrogen) for 30 min at 37°C, 5% CO<sub>2</sub>. Cells were then washed and resuspended at  $25 \times 10^3$  cells/ml in standard medium supplemented of 10% FCS and left untreated or incubated with RhoA and PKC $\epsilon$  inhibitors for 45 min at 37°C, 5% CO<sub>2</sub> before stimulation with PMA in the presence or absence of uPA. After 48 h cells were washed with warm PBS and adherent cells were fixed with warm 2% PFA/PBS for 15 min at room temperature. Intracellular actin was then stained with phalloidin-FITC (8  $\mu$ M, Sigma) in 1 ml of saponin buffer (0.1% saponin and 0.5% BSA in PBS) for 30 min at room temperature. Cells were then washed twice with warm PBS and stained with Hoechst 33342 trihydrochloride trihydrate (Invitrogen) at the concentration of 3.24  $\mu$ M in PBS for 15 min at room temperature. Cells were washed twice with PBS and maintained in PBS. Approximately 250 random fields were automatically acquired by the IN Cell Analyzer 1000 (GE Healthcare, Fairfield, CT), using objective magnification of 40 $\times$ . Analysis was performed with In Cell Investigator Software: polarized cells were identified using the “form factor”, a standard estimate of circularity that relates perimeter length to area. This measurement varies from 0 to 1, with 1 being a perfect circle. A threshold of 0.8 was fixed for this parameter and cells with a “form factor” lower than threshold classified as polarized cells. Cell polarization was based on the form factor as automatically calculated by the IN Cell Investigator Software (GE Healthcare); ratio below 0.8 was used to identify polarized cells, because was identified as the threshold discriminating between round and stretched cell shapes. Picture montage was performed by using the ImageJ software.

## Intracellular distribution of filamentous and globular actin

U1 cells were stimulated with the reported stimuli and plated on top of round coverslip. Two days later coverslips were washed twice with PBS and adherent cells fixed with 4% buffered PFA for 20 minutes at room temperature, washed twice with PBS cells and permeabilized by 0.1% Triton X-100 in PBS for 5 min at room temperature. After two more washes with PBS cells were stained with Hoechst-33342 (3.24  $\mu$ M in PBS), DNase I Alexa Fluor 488 (0.3  $\mu$ M in PBS) and phalloidin Alexa Fluor 633 (0.165  $\mu$ M in PBS) for 20 min at room temperature. After two more washes with PBS cells were mounted and sealed on microscope glass slide with Mowiol 4-88. Images were acquired by Leica TCS SP2 confocal microscope (Leica Microsystems CMS GmbH, Mannheim,

Germany) using objective magnification 63 $\times$ . Picture montage was performed by using the ImageJ software.

## Ultrastructural study

U1 cells were stimulated with PMA in the presence or absence of uPA and aliquots of  $5 \times 10^6$  cells were then washed in Phosphate Buffered Saline (PBS) and analyzed after 48 h by electron microscopy as previously described [14]. Briefly, U1 cells were washed twice in PBS, fixed in 4% (vol/vol) glutaraldehyde/2% (wt/vol) PFA/cachodilate (0.12 M pH: 7.4) and postfixed in 1% (vol/vol) OsO<sub>4</sub> (0.12 M) cachodilate buffer. Cells were dehydrated in graded ethanol, washed in propylene oxide and infiltrated for 12 h in a 1:1 mixture of propylene oxide:epoxydic resin (Epon). Cells then were embedded in Epon and polymerized for 24 h at 60°C. Slides were cut with ultramicrotome (Ultracut Uct, Leica), stained with uranyl acetate and lead citrate, and metallized.

## Protein kinase C (PKC) translocation and activation

U1 cells were washed and aliquots of  $5 \times 10^6$  cells were resuspended in 12.5 ml of RPMI 10% FCS and either left unstimulated or were stimulated with PMA in the presence or absence of uPA at the indicated time points. U1 cells were then centrifuged at 1,200 rpm for 10 min at 4°C, the culture medium was removed and the cells were resuspended in 300  $\mu$ l of cold homogenization buffer [Hepes/K (20 mM pH:7.6), EDTA/K (5 mM pH:8), EGTA/K (5 mM pH:7.6), DTT (5 mM), Na<sub>3</sub>VO<sub>4</sub> (1 mM), NaF (2 mM)] and protease inhibitor cocktail (1:1,000 vol/vol; Sigma). Cells were homogenized by 5 consecutive passages through a 22G needle mounted onto a 1 ml syringe. The cell homogenates (250  $\mu$ l) were transferred into ultracentrifuge tubes (Beckman Coulter, Fullerton, CA) and spun at 100,000 g for 60 min at 4°C (at 50,000 rpm in ultra TL-100 with the TLA-100.3 rotor or at 42,000 rpm with the TLA-55 rotor, Beckman). The supernatants containing cytosolic proteins were then collected, whereas the pellets were resuspended in 120  $\mu$ l of the homogenization buffer supplemented of 1% TritonX-100, centrifuged at 100,000 g for 30 min at 4°C (Beckman) and the supernatants containing membrane proteins were collected. Finally, 10  $\mu$ g of either cytosolic or membrane-associated proteins were loaded on 10% SDS-PAGE and analyzed by Western blotting using mAb directed against specific PKC isoforms  $\alpha$ ,  $\delta$ ,  $\epsilon$ .

Cytofluorimetric analysis of phosphorylated PKC $\epsilon$  and PKC $\delta$  was performed on cells that were washed with cold PBS, fixed with 2% PFA/PBS for 15 min at room temperature, permeabilized with saponin buffer in the presence of the specific Ab for 30 min at room temperature, followed by one wash with saponin buffer and further 30 min of incubation with the secondary anti-goat FITC Ab. An average of 15,000 cells per condition was acquired using a FACScan (Becton Dickinson, Franklin Lakes, NJ) flow cytometry apparatus and analyzed by the CellQuest software (Becton Dickinson).

## Determination of RhoA activation

The amount of the active form of RhoA (GTP-bound RhoA) was assessed using the G-LISA RhoA Activation Assay Kit (Absorbance Based; Cytoskeleton, Inc., Denver, CO) according to the manufacturer's protocol. Cell ( $5 \times 10^6$ ) were washed and resuspended in culture medium (1 ml) in the presence or absence of stimuli for the indicated time points and 10  $\mu$ g of protein were used for the assay.

## Statistics

Each experiment was design to analyze cell adhesion, clustering and polarization as well as HIV expression in the same experimental

set up. All experimental conditions were tested in duplicate wells. The results are reported as mean  $\pm$  standard deviation (SD). Multivariate analyses were conducted by one-way ANOVA and by the Tukey post-test. Differences were considered significant if  $p < 0.05$ .

## Results

### The intracellular accumulation of virions induced by uPA in PMA-differentiated U1 cells is mediated by activation of small GTPase RhoA and PKC $\epsilon$ , but not PKC $\delta$

We have previously reported that the cell adhesion-dependent antiviral signal triggered by uPA binding to uPAR requires  $\beta$ 1 and  $\beta$ 2 integrin chains [14]. We therefore investigated whether the small GTPase RhoA was mediating the intracellular accumulation of HIV virions observed upon uPA treatment of U1 cells stimulated with PMA since RhoA is known to influence cell adhesion by promoting integrin activation [32]. HIV expression from U1 cells was induced by PMA stimulation (Figure 1A and 1B), while uPA inhibited more than 50% of virus expression by promoting virion accumulation in intracellular vesicles (Figure 1C), as previously reported [14,20].

The Trojan peptides P1/23–40 and P1/92–119 were previously shown to specifically target the small GTPase RhoA [30] thus

inhibiting the transition from low to intermediate and to high affinity state and/or the lateral mobility of the  $\beta$ 2 integrin leukocyte functional antigen-1 (LFA-1, also known as CD11a/CD18), respectively. RhoA trojan peptides did not influence HIV expression in unstimulated U1 cells (data not shown) or in cells stimulated only with PMA, while they abrogated the anti-HIV activity of uPA (Figure 1A). Penetratin1 (P1), the common fusogenic component of Trojan peptides, was used as control [30].

Since protein kinase C (PKC) represents a downstream effector of RhoA [30,33], we next investigated whether activation of PKC isoforms was involved in uPA-dependent intracellular accumulation of virions in U1 cell upon PMA stimulation. Isoform-selective myristoylated pseudosubstrates peptides or control scrambled peptides were applied to U1 cells, in the presence or absence of PMA and uPA. As expected, blockade of  $\text{Ca}^{++}$ -dependent PKC $\alpha\beta\gamma$  isoforms interfered with PMA-induced virus expression in the absence of uPA, consistently with previous reports on the role of PKC activation driving HIV expression [34]. Of interest, the anti-HIV effect of uPA in PMA-stimulated U1 cells was reversed exclusively by inhibition of PKC $\epsilon$ , but not by PKC $\delta$  (Figure 1B). Ultrastructural analysis was performed on cells treated with PKC $\epsilon$  pseudosubstrate (Figure 1C and S1), showing that inhibition of PKC $\epsilon$  activation prevented both the formation of cytoplasmic vesicles as well as virion accumulation into such

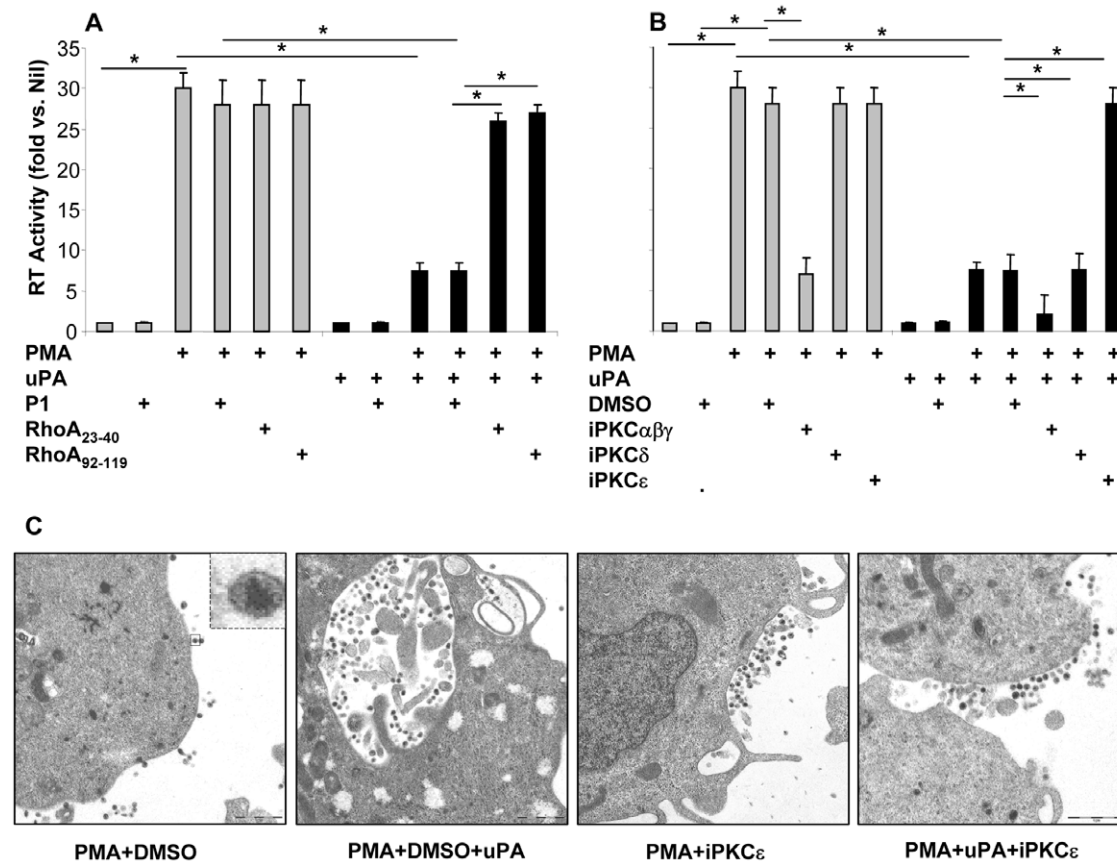


**Figure 1. The anti-HIV activity of uPA is mediated by RhoA and PKC $\epsilon$ , but not by PKC $\delta$ .** U1 cells were pre-incubated for 45–60 min at 37°C with RhoA Trojan peptide (50  $\mu$ M) (A) or myristoylated peptides specific for different PKC isoforms (50  $\mu$ M) (B) and then stimulated with PMA (10 nM) in the presence or absence of uPA (10 nM); culture supernatants were analyzed 48 h later for the levels of virus expression (mean  $\pm$  SD of 11 independent experiments). Nil represents the negative background RT activity of unstimulated U1 cells (typically, 120  $\pm$  50 cpm/ $\mu$ l). P1; penetratin was used at 50  $\mu$ M as negative control of Trojan peptides. DMSO is the vehicle in which PKC pseudosubstrate is resuspended, and here used as control. \* $p < 0.05$ . (C) Cells were stimulated in the conditions specified above and analyzed by electron microscopy 48 h after stimulation; more extensive selection of pictures is represented in the Supplementary Figures S1 and S2. iPKC; inhibitor of the specified PKC isoforms. doi:10.1371/journal.pone.0023674.g001

compartment (Table 1). In contrast, PKCε pseudosubstrate did not show any effect in U1 cells stimulated with interleukin-6 (IL-6) (Figure S2), a cytokine triggering HIV expression in U1 cells without inducing cell adhesion and, therefore, insensitive to the inhibitory effects of uPA [15].

All above inhibitors were used at concentrations that provide the maximal biological effect in the absence of evident cellular toxicity, as determined by cell proliferation (measured in terms of overnight uptake of <sup>3</sup>H-thymidine) and cell viability (by Trypan-blue dye exclusion) [19] after 3 days of stimulation. A PKCζ pseudosubstrate was also tested, but resulted in either toxic effects on the cells or in no effect on cell adhesion when used at non-toxic concentrations (data not shown).

### uPA-induced cell adhesion and cell polarization is mediated by small GTPase RhoA, PKCδ and PKCε

PMA stimulation of myelo-monocytic cell lines, including promonocytic U937 and U1 cell lines, induce their activation and differentiation along the macrophage lineage [26]. Such a process is associated with the transition from cell proliferation in suspension to a drastic decrease of the proliferative capacity and acquisition of cell adhesion to the substrate. As we have previously demonstrated in primary MDM [15], PMA-induced U1 cell adhesion to the substrate was enhanced in the presence of uPA (Figure 2A). Although both RhoA Trojan peptides failed to affect PMA-induced cell adhesion; however, they fully prevented the enhancement of adhesion to the substrate induced by uPA (Figure 2A).

Next, we investigated whether activation of PKC isoforms was involved in uPA-dependent increase of U1 cell adhesion following PMA stimulation. In this regard, different studies have reported that both PKCα and ζ regulate, concurrently with RhoA, β<sub>1</sub> and β<sub>2</sub> integrin-dependent adhesion resulting in cell spreading and lateral mobility of LFA-1, respectively [30,35]. As in the case of HIV expression, blockade of Ca<sup>++</sup>-dependent αβγ PKC isoforms also interfered with PMA-induced cell adhesion (Figure 2B). Furthermore, it has been reported that both uPA and ATF can lead to formation of diacylglycerol (DAG) that, in turn, can induce the activation of PKC δ and ε isoforms [36] associated with promotion of cell adhesion and migration of human epithelial cells [37,38]. Consistently, pharmacological targeting of PKC δ and ε isoforms did not influence PMA-dependent cell adhesion but fully prevented its enhancement induced by uPA (Figure 2B).

Concomitantly with the enhancement of cell adhesion, uPA inhibited homotypic cell aggregation, as reported [15]. PMA induced formation of both adherent cells and of cell aggregates

that remained in suspension (Figure S2). Cell aggregation was abolished and all cells were adherent to the substrate when co-stimulated with PMA and uPA (Figure S2A). Trojan peptides targeting the small GTPase RhoA did not modify PMA-induced cell clustering but fully reversed the inhibitory effect of uPA (Figure S3A). PMA-induced homotypic clustering of U1 cells was not affected by the PKC pseudosubstrates tested (Figure S3A–B). In addition, interference with PKC δ or ε, but not with the αβγ isoforms, reversed the uPA-dependent inhibition of cell aggregation (Figure S3B).

In parallel to the induction of cell adhesion (and to the prevention of cell aggregation) uPA induced a morphological polarization of U1 cells, as previously observed in the case of neutrophils [39], vascular smooth muscle and epithelial cells stimulated by uPA or ATF [37]. Polarized cells were characterized by the formation of classical uropods (Figure 3A and Figure S4) that were only present in adherent cells. This change in cell shape was still observed 48 h after stimulation. This finding is in accordance to previous findings showing that binding of uPA to uPAR on the surface of U937 cells is long-lasting, with ca. 80% of input uPA bound to uPAR after 4 h [40]. Furthermore, uPA proteolytic activity in the monocytic cell line THP-1 has been shown to last for 40 h or longer [40]. Uropods formation was indeed not observed when cells were cultivated in ULA plates (data not shown), characterized by low binding of serum proteins and lack of cell adhesion [15]. Unbiased quantification of the number of polarized cells was performed on randomly selected fields acquired by InCell analyzer (Figure 3A), with the cells being analyzed for their width/length ratio by the InCell Investigator software excluding from the analysis cells partially out of the field (Figure S5). As observed by phase contrast microscopy (Figure S4), the InCell Investigator software quantified that 4.7% and 15% of the adherent U1 cells were indeed polarized after PMA or PMA+uPA, respectively (Figure 3B). Furthermore, PMA-stimulated U1 cells were characterized by the absence of uropods, whereas co-stimulation with PMA and uPA induced a more evident cell polarized characterized by a lower width/length ratios and induced the formation of uropods (Figure 3B). Inhibition of RhoA or PKCδ or PKCε activities did not affect PMA-induced cell polarization (data not shown) but abolished the enhancement of cell polarization induced by uPA to values similar to those observed in PMA-stimulated cells (Figure 3C). In contrast, RhoA Trojan peptides did not show any effect in U1 cells stimulated with interleukin-6 (data not shown), a cytokine triggering HIV expression in U1 cells without inducing a macrophage-like phenotype, therefore insensitive to the inhibitory effects of uPA [15].

**Table 1.** PKCε and virion partitioning in stimulated U1 cells.

Stimuli	p.m.-associated virions	i.c. virions	% virions pm/ic	# vesicles per cell	# cells with vesicles/total
PMA	74	0	100	1	1/10
PMA+iPKCε	199	3	98	2	2/10
PMA+uPA	58	79	42	>10	9/10
PMA+uPA+iPKCε	165	5	97	1.5	5/10
IL-6	46	0	100	0	0/10
IL-6+iPKCε	105	0	100	0	0/10

U1 cells were pretreated with PKCε pseudosubstrate and stimulated for 48 h with the indicated stimuli, and analyzed by transmission electron microscopy as previously reported [14]. Unstimulated U1 cells did not show evidence of either virion production or cell vacuolization (not shown). p.m.: plasma membrane; i.c.: intracellular; iPKCε: inhibitor of the isoform PKCε.

doi:10.1371/journal.pone.0023674.t001

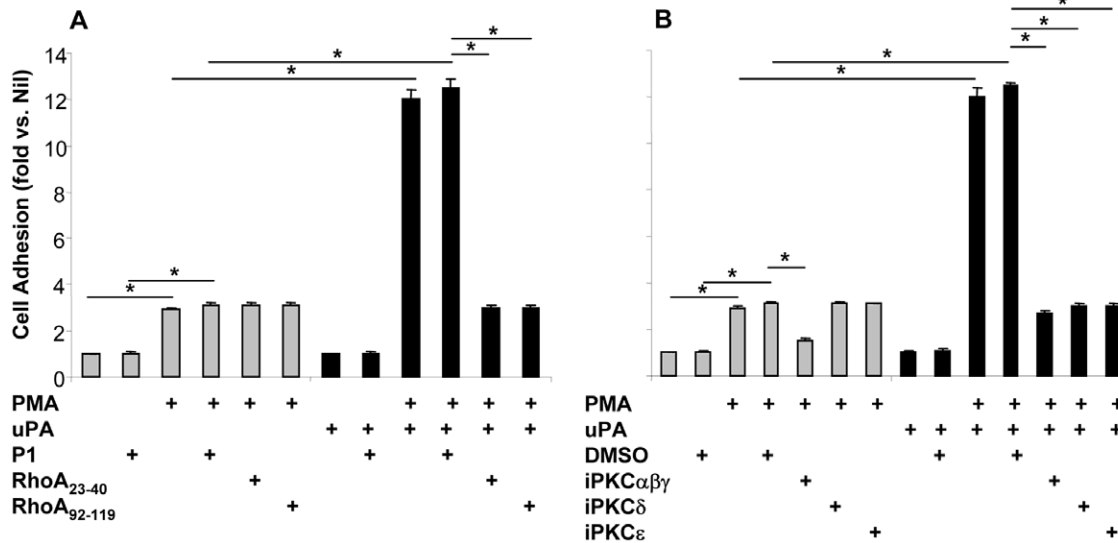


**Figure 2. uPA induces adhesion of PMA-differentiated U1 cells via activation of small GTPase RhoA, PKCδ and PKCε.** U1 cells were pre-incubated for 45–60 min at 37°C with RhoA Trojan peptide (A) or myristoylated peptides specific for different PKC isoforms (B) and then stimulated with PMA in the presence or absence of uPA; cells were analyzed 48 h later for their capacity to adhere to the plastic substrate. uPA increased the adhesion of PMA-stimulated U1 cells and this effect was reversed by inhibition of either RhoA or different PKC isoforms. Results are shown as mean  $\pm$  SD of 11 independent experiments. Nil indicates unstimulated U1 cells, showing a mean net absorbance value (subtracted of the background value of an empty well) of  $0.07 \pm 0.012$ . \* $p < 0.05$ . doi:10.1371/journal.pone.0023674.g002

#### uPA induces actin rearrangement in PMA stimulated U1 cells

Since both cell adhesion and polarization are dependent on cytoskeleton re-organization, intracellular distribution of globular (G) and filamentous (F) actin was investigated. Two days after PMA or PMA+uPA stimulation adherent U1 cells were stained with probes specific for G and F actin, such as DNaseI and phalloidin, respectively. In PMA-stimulated U1 cells G actin was homogeneously distributed, with F actin was localized below the cellular membrane (Figure 4A) when U1 cells were stimulated by PMA in the presence of uPA G actin was homogeneously distributed (Figure 4B), although levels of intensity were decreased (Figure 4B and Figure S7A). However, uPA did not alter actin expression [14] indicating that decreased levels of G actin intensity are consequent of G to F switch, likely due to an increased volume of uPA stimulated cells (Figure 3A and Figure S7A). Indeed, distribution of F actin in PMA+uPA stimulated cells overlapped to that observed in PMA stimulated cells, such as below the cellular membrane, but also in tails present only in polarized cells (Figure 4B).

#### uPA induces RhoA activation in PMA stimulated U1 cells

In order to assess the activated form of RhoA we measured the GTP-bound form of RhoA by G-LISA. Unstimulated (Nil) and PMA-stimulated cells showed equal levels of activated RhoA (Figure 5A), confirming independent studies indicating that PMA failed to activate RhoA in fibroblasts [41]. In contrast, uPA induced RhoA activation in both unstimulated and PMA-stimulated U1 cells (Figure 5A and 5B). RhoA activation reached a peak of activation as soon as 5 min after uPA stimulation, returning to basal levels after 60 min (Figure 5A and 5B). It should be underscored that U1 cells at these early time points are still completely in suspension, and that the same findings were observed in ultra-low adhesion (Teflon-coated) plates (data not shown).

The levels of RhoA activation were also analyzed after 24 and 48 h of culture. When both unstimulated and PMA-stimulated cells were maintained in suspension in Teflon-coated plates the levels of RhoA activation were constant over time (from 5 min to 48 h, Figure 5A and 5C, dashed lines), whereas it decreased by  $\sim 6$  folds after 24–48 h in standard plates allowing cell adhesion (Figure 5C and 5D), as described [32]. In contrast, uPA stimulation caused an increased in RhoA activation exclusively in cells that were allowed to adhere, but not in cells cultivated in Teflon-coated plates, as observed after 24–48 h of culture (Figure 5C and 5D). Thus, a second wave of RhoA activation, likely consequent to integrin outside-in signaling, is generated and maintained upon uPA-induced cell adhesion.

#### uPA induces activation of PKC ε and δ isoforms

We measured the activation of PKC isoforms in terms of their translocation from the cytoplasm to the membrane [42] (Figure 6A) as well as of the presence of phosphorylated isoforms (Figure 6B). As expected, PMA induced the complete translocation of PKCα from the cytosol to the plasma membrane as tested 10 min after cell stimulation (Figure 6A), an event that was unaffected by uPA (data not shown). PKCε was detected exclusively in the cytosolic fraction of unstimulated U1 cells while PMA poorly induced its translocation to the plasma membrane (Figure 6A). Stimulation of U1 cells with uPA alone induced a time-dependent PKCε translocation to the membrane (Figure 6A). When cells were co-stimulated with PMA and uPA, however, a synergistic effect was observed on the translocation of this PKC isoform from the cytosol to the membrane that was already maximal 10 min after stimulation and remained elevated for at least an additional 50 min.

In comparison to PKCε PKCδ showed faster kinetics of translocation from the cytosol to the plasma membrane that was already maximal 10 min after stimulation with uPA in the absence of PMA (Figure 6A). Like PKCε, also for PKCδ the strongest

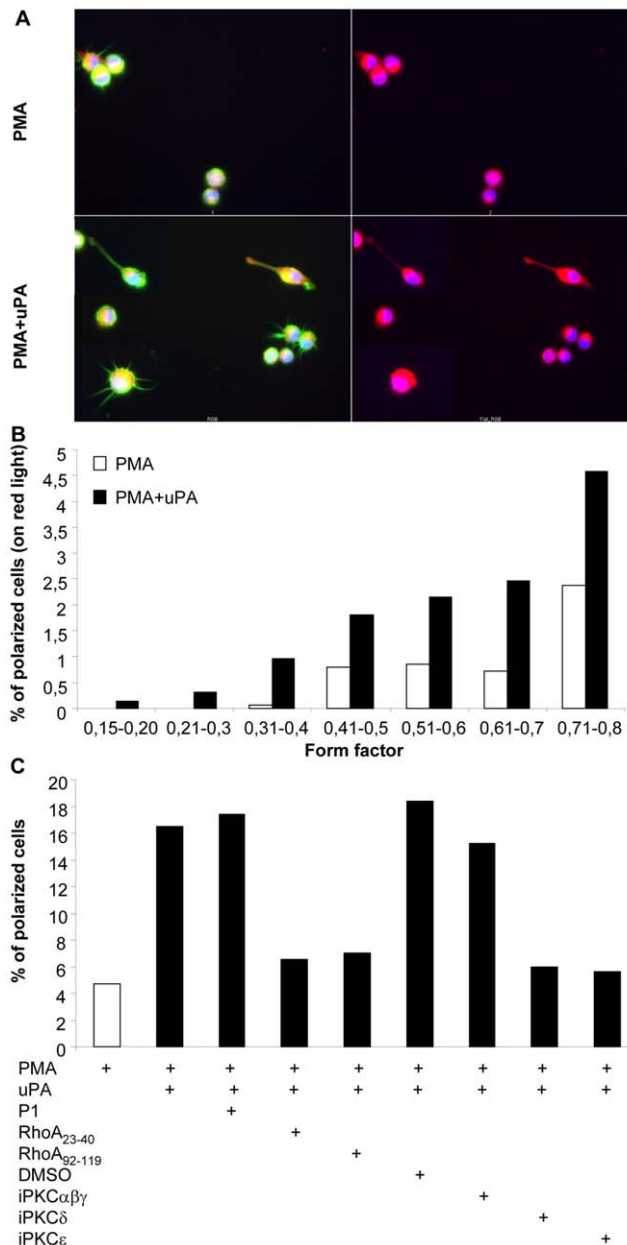


**Figure 3. uPA induces polarization of PMA-differentiated U1 cells.** U1 cells were loaded with cell tracker (red color) and then stimulated with PMA in the presence or absence of uPA. Adherent cells were stained 2 days later for F-actin (phalloidin-FITC, green color) and nuclei (blue color). A total of 1,142 and 2,245 adherent cells were counted after stimulation with either PMA alone or in the presence of uPA, respectively. **(A)** uPA induces polarization of U1 cells with formation of uropods, not observed in control cells stimulated only with PMA. **(B)** Quantification and distribution of polarized cells, as defined by form factor <math><0.8</math>. **(C)** Inhibition of anti-RhoA or PKC  $\delta$  and  $\epsilon$  isoforms reverted uPA-induced cell polarization: this analysis is based on the distribution of the cell tracker (right panels, red light) since staining of F-actin (left panels, green light) revealed the presence of filopodia, cell surface projections highly enriched in F-actin required for the formation of focal adhesion sites [73] that may produce false-positive results. doi:10.1371/journal.pone.0023674.g003

activation was induced by simultaneous co-stimulation of U1 cells with PMA and uPA. This pattern is likely explained by the observation that PMA has been shown to enhance uPAR affinity for uPA, either directly or indirectly affected by PKC [43].

Since membrane fractionation does not allow isolation of plasma membrane from total membranes, a second method for analyzing PKC activation was used, and intracellular levels of activated isoforms was performed by cytofluorimetric analysis. U1 cells stained negative for activated PKC $\epsilon$ , whereas 30 min of stimulation with either PMA alone or uPA poorly induced its phosphorylation. However, PMA+uPA stimulation induced phosphorylation of PKC $\epsilon$  in most cells (Figure 6B). Related to activated PKC $\delta$  PMA did not induce appreciable activation, whereas cell stimulation with either uPA alone or in the presence of PMA increased the number of cells positive for phosphorylated PKC $\delta$  (Figure 6B).

### Cytochalasin D (CytD) mimics the anti-HIV activities of uPA in PMA-stimulated U1 cells

We have previously reported that both  $\beta_1$  and  $\beta_2$  integrin chains mediate the antiviral effect of uPA in PMA-stimulated U1 cells as well as that integrin activation in the absence of uPA led to a similar effect [19]. Since integrin function is linked to the cytoskeleton activity we investigated the potential role of cytoskeletal elements in HIV expression and uPA-dependent effects. Therefore, U1 cells were stimulated in the presence or absence of CytD, a cell-permeable fungal toxin that prevents F actin polymerization and induces RhoA activation [32].

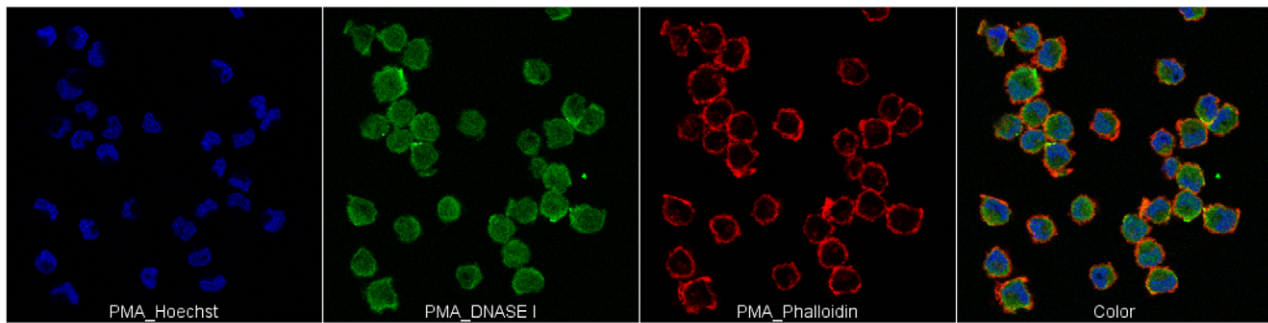
CytD did not influence the basal undetectable levels of virus expression in unstimulated U1 cells (Figure 7A), but it inhibited HIV release in PMA-stimulated cells to an extent comparable to that induced by uPA (Figure 7A). We next freeze-fractured CytD-treated cells and observed an increase in RT activity reaching levels to those of control PMA-stimulated cells, similar to what observed with uPA (Figure 7B), suggesting that the anti-HIV activity of CytD, as described for uPA [14], likely results in the intracellular budding and accumulation of virions; indeed, independent studies reported that CytD did not inhibit HIV proteins expression and maturation but HIV virion release in monocytic and T cell lines (U937 and Jurkat, respectively) [44,45].

Consistently with independent findings [32,46], we observed activated RhoA after 30 min of CytD incubation, an effect that lasted for at least 2 h, independently of the presence of PMA (Figure 7C). Similarly to what observed in uPA-stimulated cells (Figure 5A) the levels of RhoA activation were enhanced of about 50% (Figure 7D). Furthermore, CytD induced adhesion of unstimulated U1 cells, as reported for other cell types [47], and this effect was additive in the presence of PMA (Figure 7E).

CytD induced polarization of U1 cells, as reported on other cell types [47,48], and also this effect was dependent upon PKC $\epsilon$  activation (Figure 8A). CytD induced cell polarization as soon as after 15 min of stimulation and independently of cell adhesion. Moreover, like uPA, CytD also prevented the formation of cell aggregates in PMA-stimulated cells after 48 h of stimulation, another effect that was prevented by inhibition of PKC $\epsilon$  activation (Figure 8A). We have also analyzed distribution of G and F actin in CytD adherent cells. As previously reported in fibroblasts [49], F actin resulted to be localized in focal aggregates (Figure 8B, middle panels), excluded from tails present in polarized cells. G actin was broadly distributed and also present in tail of polarized cells (Figure 8B, middle panels). PMA+CytD stimulated U1 cells were characterized by a morphology similar to that observed with CytD alone, although increased levels of intensity of F actin were noticed, probably due to the additive adhesion effect induced by PMA and CytD (Figure 8B, bottom panels and Figure S6B).

As in U1 cells stimulated with PMA+uPA, CytD-induced cell adhesion was dependent on RhoA and PKC $\epsilon$  activation (Figure 7E). Noteworthy, however, unlike uPA, the anti-HIV

A



B

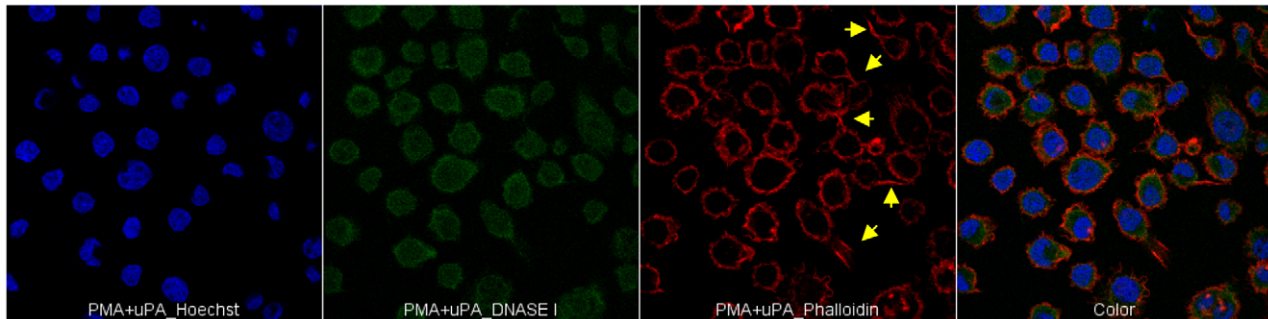


**Figure 4. Different actin distribution in uPA polarized cells.** U1 cells were stimulated with PMA in the presence or absence of uPA and actin distribution in adherent cells was visualized by confocal microscopy after 48 h of culture. Hoechst-33342, DNase I (Alexa Fluor 488, green) and phalloidin (Alexa Fluor 633, red) were used to discriminate nuclei, globular (G actin) and filamentous (F actin) isoforms, respectively. Images were acquired with 63 $\times$  magnification by Leica TCS SP2 confocal microscope (Figure S6) and electronically zoomed 3 times. Image J software was used to perform montage of the three colors. Yellow arrows indicate polarized cells. One experiment out of three independently performed with similar results is shown. doi:10.1371/journal.pone.0023674.g004

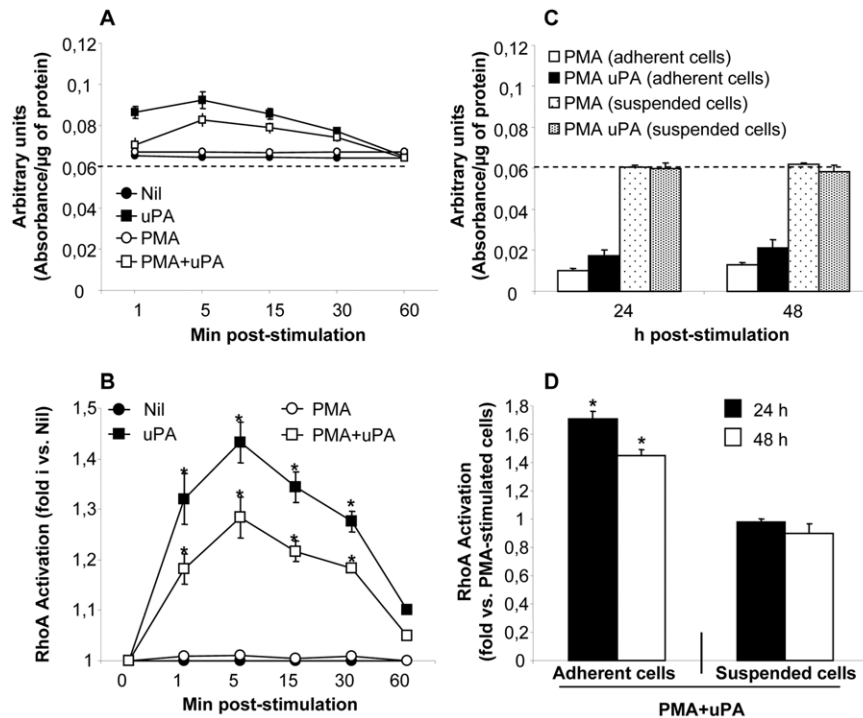


**Figure 5. uPA induces two waves of RhoA activation in PMA-activated U1 cells.** Quick RhoA activation in U1 cells upon uPA stimulation: absorbance indicating RhoA activation was measured by the G-LISA kit assay and was normalized per  $\mu$ g of protein (A) and results of 3 independent experiments reported ad fold induction (mean  $\pm$  STD) vs. unstimulated cells (B). Delayed uPA-induced activation of RhoA is adhesion-dependent: RhoA activation was measured in PMA or PMA+uPA stimulated U1 cultivated in culture plates (adherent cells) or in Teflon-coated plates not allowing adhesion (suspended cells) (C), and results of 3 independent experiments reported ad fold induction (mean  $\pm$  STD) vs. PMA stimulated cells. The dotted line in panels A and C indicate the levels of RhoA activation observed in unstimulated cells (panel A) and in cells maintained in suspension in ULA plates after stimulation for 24–48 h with PMA (C). Calpeptin (2 U/ml for 15 min) was used as positive control and induced  $2 \pm 0.1$  fold of RhoA activation vs. Nil (not shown). doi:10.1371/journal.pone.0023674.g005

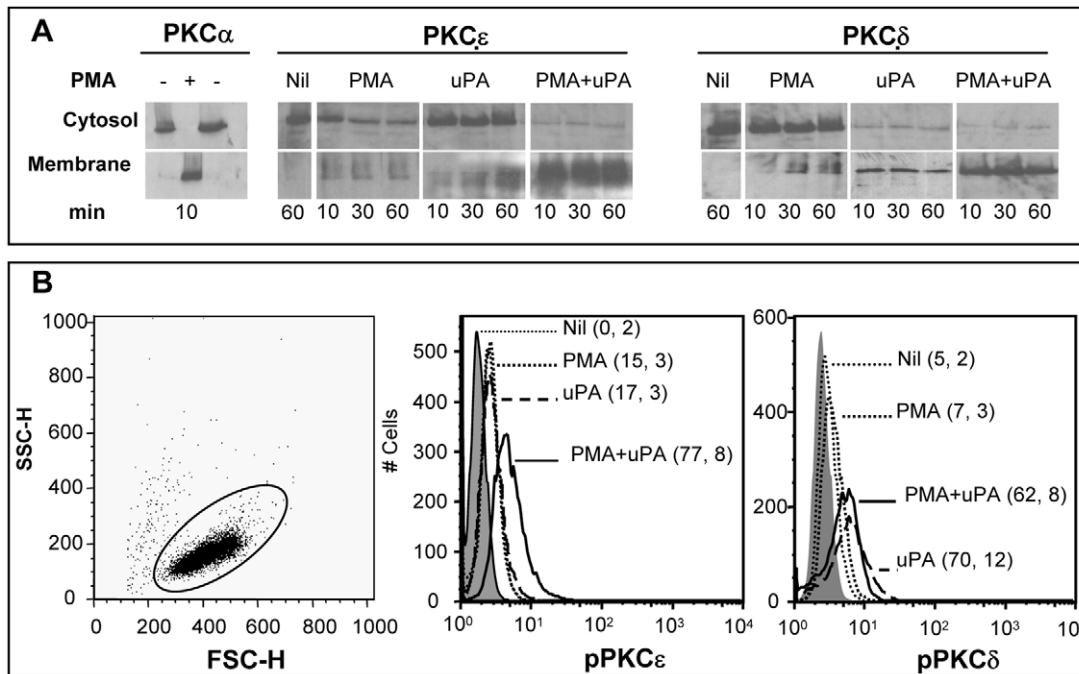


**Figure 6. uPA induces activation of PKC $\delta$  and  $\epsilon$  in PMA-stimulated U1 cells.** PKC activation was measured by two independent assays, such as cytosol-membrane translocation of PKC and measurement of PKC isoforms phosphorylation. Cells were left either unstimulated or were incubated with PMA in the presence or absence of uPA. **(A)** Membrane and cytosolic fractions of U1 cells were analyzed for the presence of PKC isoforms at the indicated time points; membrane and cytosolic extracts were run independently but in a single gel per fraction. **(B)** Cells were analyzed by cytofluorimetric means for the presence of phosphorylated PKC $\epsilon$  and PKC $\delta$  30 min after stimulation (numbers in parentheses represent the % of positive cells and geometric means of fluorescence, respectively). The results shown in A and B were obtained from a single experiment representative of 5 independently performed. doi:10.1371/journal.pone.0023674.g006

activity of CytD was not dependent on cell adhesion since superimposable results were obtained in Teflon-coated plates preventing cell adhesion (Figure 7F).

## Discussion

In the present study, we have investigated the signaling determinants involved in uPA-dependent inhibition of HIV-1 expression in a well defined model of macrophage infection such as chronically infected promonocytic U1 cells activated and differentiated by PMA. Indeed, several features typical of primary macrophage infection are observed in PMA-stimulated U1 cells, including the shift from growth in cell suspension to firm adhesion to the substrate coinciding with growth arrest [15] and the expression of the CD11b integrin chain [19], as also reported in the U1 uninfected parental cell line U937 [43]. Morphologically, PMA-differentiated U1 cells acquire a macrophage-like phenotype characterized by a ruffled plasma membrane and a vacuolarized cytoplasm where HIV frequently buds into and accumulate, particularly when IFN- $\gamma$  or uPA are applied together with PMA [14,23]. Finally, PMA-stimulated U1 cells resembles human MDM in terms of secretion of uPA, soluble uPAR (suPAR) and suPAR/uPA ratio [19].

Both the small GTPase RhoA and DAG-activable PKC isoforms  $\delta$  and  $\epsilon$  were activated by uPA. Along with increased U1 cell adhesion and inhibition of homotypic cell clustering, uPA induced polarization of PMA-stimulated U1 cells and RhoA activation. However, only RhoA and PKC $\epsilon$  were linked to the intracellular accumulation of HIV virions, while uPA-dependent increased cell polarization and adhesion were dependent on

RhoA, PKC $\delta$  and PKC $\epsilon$ . CytD recapitulated through different dynamics all the essential features of uPA-dependent modulation, such as U1 cell adhesion, polarization and prevention of HIV virions release.

The uPA/uPAR complex has been involved in multiple biological processes and its dysregulation has been linked to important pathological conditions, including the formation of cancer metastasis and HIV/AIDS disease progression [3]. uPA activities can be subdivided in those processes consequent to its proteolytic component from those occurring after signaling mediated by uPAR association with a transducing receptor. The modulatory effects here investigated are strictly associated with this "second life" of uPA, such as cell adhesion, polarization and anti-HIV activity [14,20]. uPA-induced chemotaxis of human vascular smooth muscle cells was reported to be mediated by activation of small GTPase RhoA and downstream phosphorylation of myosin light chain [50]. In this regard, the small GTPase RhoA has been previously implicated in chemoattractant-induced  $\beta_1$  [51] and  $\beta_2$  integrin mediated leukocyte adhesion, and, particularly, for  $\alpha_L\beta_2$  (LFA-1), in the regulation of heterodimer affinity increase and lateral mobility [30,52], as well as in the enhancement of monocyte and promonocytic U937 cell adhesion to the substrate [53,54] and very recently of neutrophil adhesion on fibrinogen [55].

Consistently, our previous [15] and current findings link them to the anti-HIV effect of uPA in various models of macrophage infection (including primary MDM and PMA-differentiated U1 cells) to an increased cell adhesion and to the activation of RhoA. Of interest is the fact that an inhibitory effect of transfected RhoA on HIV gene transcription and replication was demonstrated to

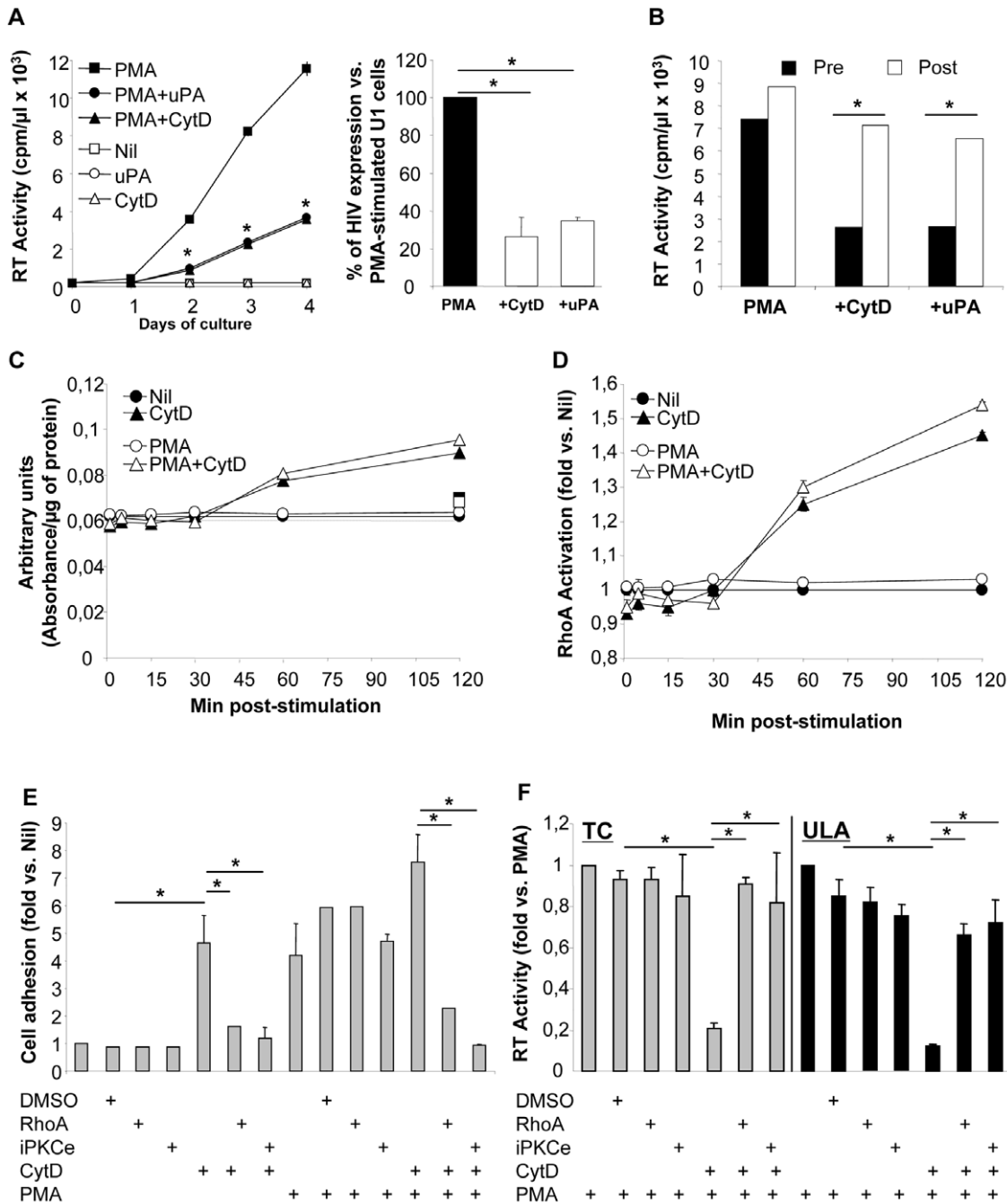


**Figure 7. CytD inhibits late phase of HIV expression via activation of small GTPase RhoA and PKCε.** (A) U1 cells were resuspended in culture medium supplemented with either CytD (10 μM) or 10 nM uPA and then left unstimulated or stimulated with PMA. Kinetics (left panel) and % of inhibition after 48 h of stimulation (right panel) are shown from 1 experiment representative of 4. (B) RT activity was measured after 72 h of stimulation in the supernatant of cells before and after being subjected to cycles of freezing and thawing. The results from 1 experiment out of 2 independently performed are shown. (C) RhoA activation in U1 cells upon CytD stimulation: absorbance indicating RhoA activation was measured by the G-LISA kit assay and was normalized per μg of protein. (D) Results of 3 independent experiments reported as fold induction (mean ± STD) vs. unstimulated cells. (E) U1 cell adhesion was measured after 48 h of stimulation; the results are represented as fold induction vs. unstimulated cells (Nil; with net OD values, subtracted of background, ranging between 0.05–0.06). (F) The RT activity was measured in the culture supernatants after 48 h of stimulation; the results are represented as fold of induction vs. PMA-stimulated U1 cells (with values ranging between 2,500–3,000 cpm/μl in standard plates (TC, tissue culture) allowing cell adhesion and 8,000–10,000 cpm/μl in ultra-low adhesion (ULA) plates, as reported [15]. Panels (E) and (F) show the average ± SD of 4 independent experiments; control peptides, such as P1 and scrambled PKC pseudosubstrate produced results superimposable to those of DMSO. \*p<0.05. doi:10.1371/journal.pone.0023674.g007

occur in both adherent CD4-expressing 293T cells and in non-adherent Jurkat T lymphocytic cells [56]. In contrast, a positive role of RhoA activation has been described in dendritic cells

following DC-SIGN activation and formation of an immunovirological synapse with T cells [57]. However, these two seemingly opposite effects may in fact represent two consequence of the same

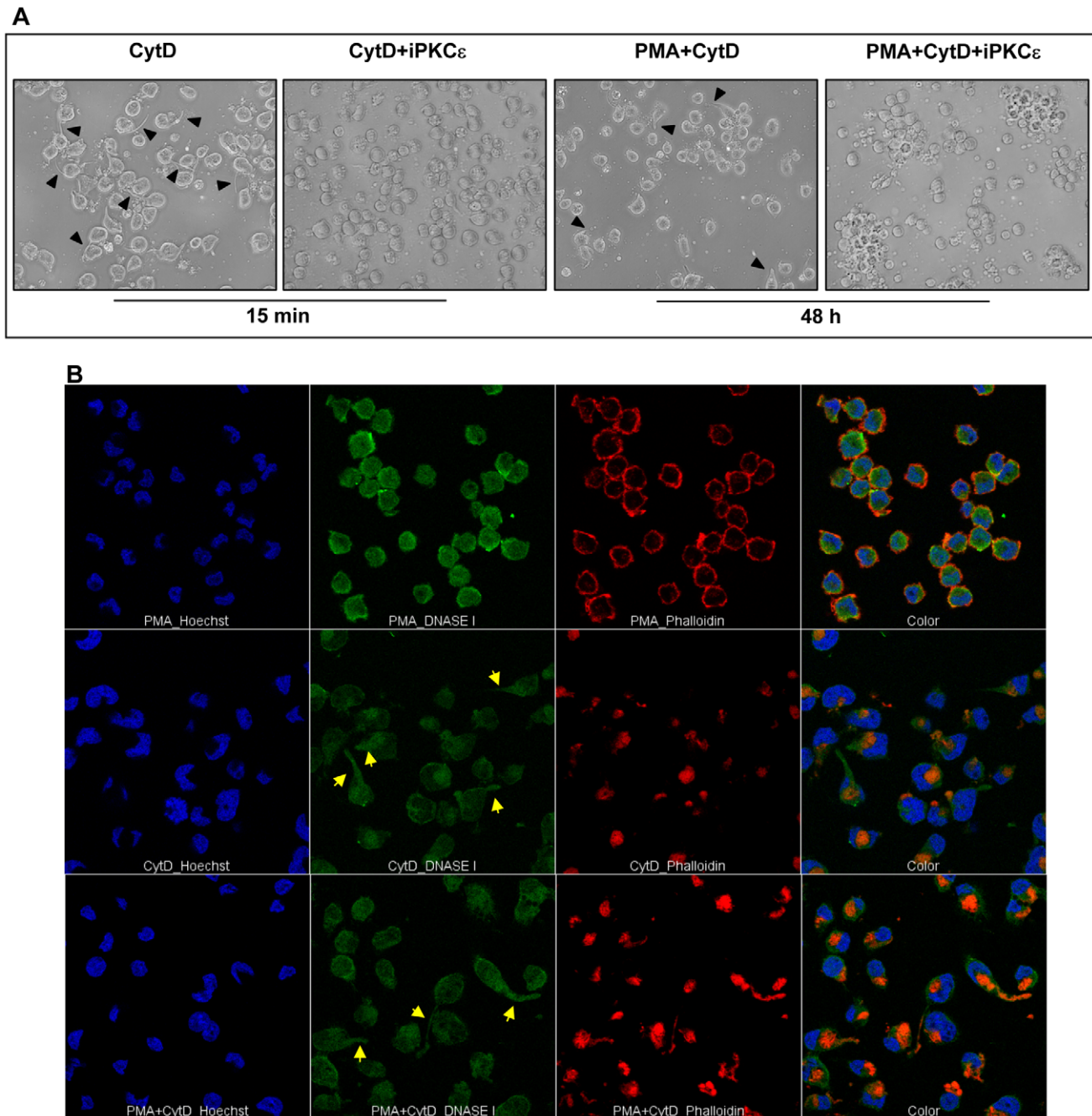


**Figure 8. CytD induces U1 cell polarization and modification of actin distribution.** U1 cells were stimulated with CytD in the presence or absence of PMA. **(A)** U1 cells were pre-incubated for 45–60 min at 37°C with the PKC $\epsilon$  inhibitor and then stimulated with either CytD or CytD+PMA; cell polarization was visualized 15 min and 48 h after stimulation. Phase contrast pictures of cells were shot at 20 $\times$  magnification; arrowheads indicate polarized structures. **(B)** G and F actin distribution in adherent U1 cells; upper panels show the effect of PMA stimulation, middle panels those of CytD stimulation and bottom panels of PMA+CytD co-stimulation. Staining of G and F actin, image acquisition and montage were performed as describe in the Figure 4 legend. Yellow arrows indicate polarized cells. One out of 3 independent experiments performed with similar results is shown.

doi:10.1371/journal.pone.0023674.g008

biological phenomenon: the concentration of virions in intracellular vesicles that could represent an inhibitory outcome for free virion release, but facilitate cell-cell virion transmission.

Downstream to RhoA [30,33], activation of PKC is crucial for modulation of several cellular processes. In this regard, activation of PKC isoforms influences the morphology of the F-actin cytoskeleton and thereby regulates processes that are affected by

remodeling of the microfilaments [42]. Integrins are crucial mediators both upstream and downstream of PKC in inducing morphological changes [42]. In addition, HIV virions and cytoskeleton elements strongly interact each other after the entry step or in order to bud from the infected cell as also evidenced by the incorporation of actin and actin-binding molecules into virions [58,59]. Thus, PKC activation may lead to the regulation of virus

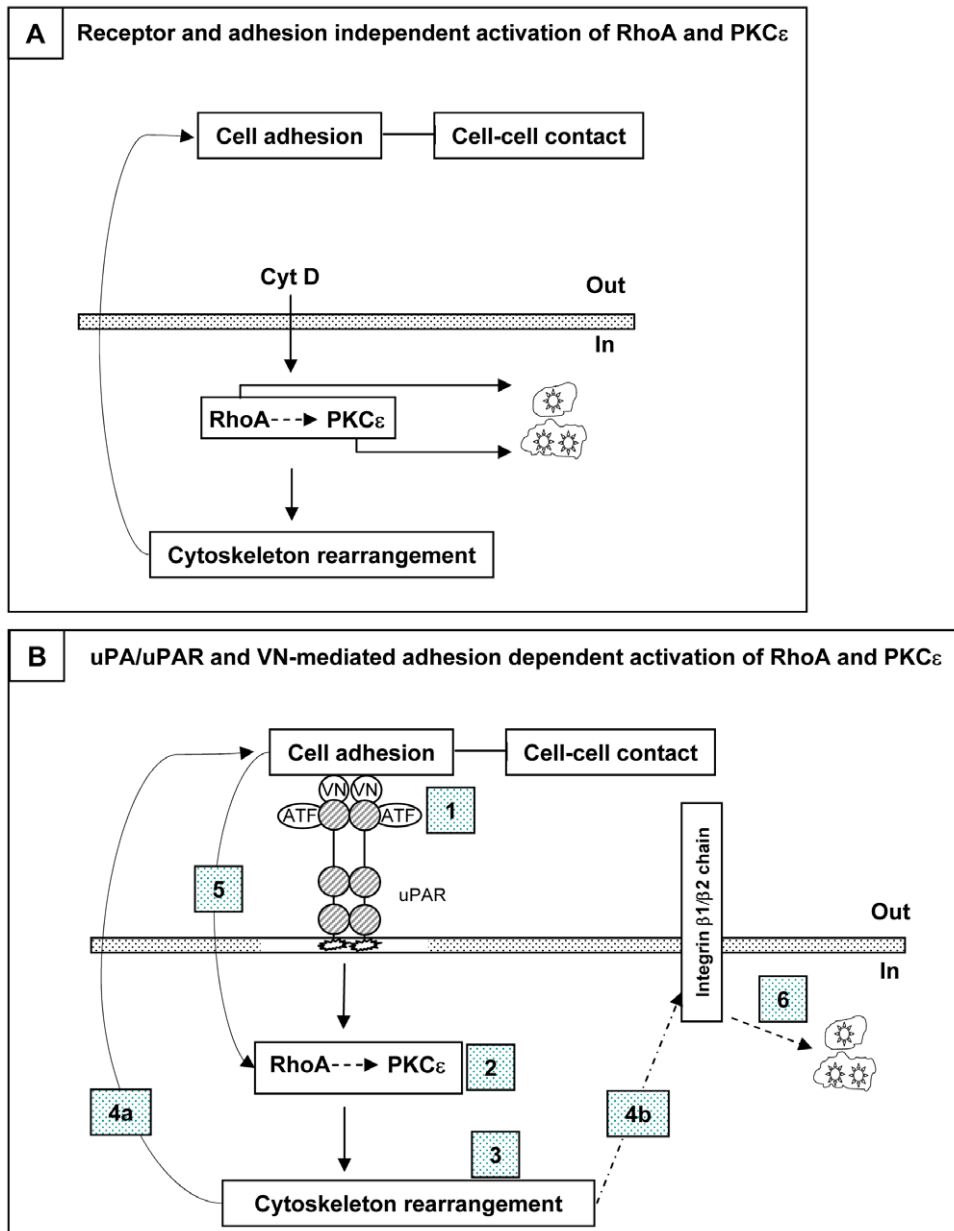


**Figure 9. RhoA and PKC $\epsilon$  activation leads to accumulation of HIV virions in cytoplasmic vacuolar compartments.** (A) CytD mediated accumulation of virions is reversed by blocking RhoA and PKC $\epsilon$  independently of cell adhesion. The same enzymes also modulate cytoskeletal rearrangement, as evident by cell polarization shown in Figure 8 and promote cell adhesion and inhibition of cell clustering [74]. (B) Binding of the signaling-competent portion of uPA (ATF) to uPAR recruits VN [15,75] leading to dimerization of the complex likely occurring in lipid rafts [76] (white box inside the dashed box representing cell membrane, whereas stars represent GPI-anchor associated to uPAR) (step 1), independently of integrin activation [77], followed by early activation of RhoA and then PKC $\epsilon$  (step 2). Cytoskeleton is rearranged (step 3) leading to two events, such as i) reinforcement of cell adhesion (step 4a) [32,78] generating a second wave of RhoA activation (step 5), and ii) activation/clustering of  $\beta_1$  and  $\beta_2$  integrin chains (step 4b) [19] therefore generating a signaling cascade leading to the intracellular accumulation of virions in intracellular vesicles (step 6). Full arrows represent our experimental findings, whereas dashed arrows are hypothetical. doi:10.1371/journal.pone.0023674.g009

expression either directly, by influencing viral transcription [60,61] or by phosphorylating viral proteins [62], or indirectly via induction of cytoskeleton rearrangement. In particular, PKC $\epsilon$  has been shown to phosphorylate vimentin (VM) [63] a cytoskeleton protein important for the cytoplasmic localization of the viral accessory protein Vif [64], therefore affecting virion infectivity [65]. VM activation can trigger the association of vesicle-bearing  $\beta_1$  integrins to intermediate filaments, thus

allowing their movement towards the plasma membrane [63]. uPA-mediated activation of PKC $\epsilon$  might regulate VM activity by altering its interactions with Vif and the viral protease [66] ultimately resulting in the accumulation of virions in intracellular vacuolar compartments. In this regard, blocking events downstream to PKC $\epsilon$  erased the ability of uPA to induce intracellular vacuolization, a marker of functionally mature phagocytes [67]. Overall, these findings suggest that uPA-induced activation of

PKC $\epsilon$  is involved in pathways of host proteins stored into vesicles (i.e., needed for recycling of membrane receptors during chemotaxis), a system reported to be exploited by HIV in infected macrophages [68].

In order to better define the role of cytoskeleton in uPA-mediated activities, we also studied the effect of Cytochalasin D, a cell-permeable compound that does not require interaction with any membrane receptor to mediate both RhoA activation and cytoskeleton remodeling. CytD has been reported that it binds to the barbed end of G actin thus preventing the following polymerization to F actin and leading to the accumulation of G actin. Moreover, it has been reported that F actin sequesters Rho guanine-nucleotide exchange factor, thus abrogating RhoA activation [69]; indeed, also microtubule disruption with either nocodazole or colchicines has been reported to increase global RhoA activity in neutrophils [70]. Consistently with this model we observed increased levels of activated RhoA upon 30 min of incubation, as reported independently [32,46], after cytoskeletal rearrangement, an event that occurred as soon as after 15 min of treatment. Indeed, inhibition of RhoA reversed CytD-induced cell adhesion and inhibition of HIV release. Nonetheless, cell adhesion, polarization and inhibition of HIV release induced by CytD were also mediated by PKC $\epsilon$ , an enzymatic activity reported to be downstream of RhoA-mediated signaling. Thus, a potential model of uPA/uPAR interaction may include the generation of an intracellular signal of reorganization of cytoskeleton components similar to that induced by CytD (Figure 9A) that inhibits virus replication at the level of virion assembly and release [45].

A potential working model connecting the multiple events induced by the uPA/uPAR system is shown in Figure 9B. According to this model, uPA/uPAR/VN complex likely triggers an outside-in signaling cascade facilitating cell adhesion and polarization of adherent cells. Since cell polarization occurred exclusively in adherent cells, but not in cells maintained in suspension in ULA plates, the intracellular signaling triggered by uPA, involving the activation of RhoA and PKC  $\delta$  and  $\epsilon$ , is crucial for the acquisition of cell polarity (i.e. formation of the uropods and, eventually, pseudopods), as previously discussed for epithelial cells [37], needed for migration on substrate. Conversely, the VN/uPA/uPAR complex might generate an “inside-out” signaling by perturbing the cytoskeleton organization triggering integrin activation that, in turn, may trigger an “outside-in” signaling pathway leading to cell polarization, as reported for CXCL12-dependent integrin activation, reported to induce cell adhesion and migration via activation of RhoA followed by activation of the integrin LFA-1 [41,71,72].

Thus, the uPA/uPAR/VN system favors macrophage adhesion and accumulation of virions in intracellular vesicles [68], highlighting a potential mechanism for the establishment and maintenance of this intra-cytoplasmic reservoir of preformed virions. Such a feature of virion morphogenesis has generated the model of macrophages as “Trojan horses” of infection, hiding infectious virions from the recognition of immune effectors such as neutralizing antibodies [68]. Finally, our results also extend uPA/uPAR-related findings to a broader model that involves pathways controlling cytoskeleton remodeling and activation of RhoA and PKC $\epsilon$  as mediators of intracellular accumulation of HIV virions in vesicles as well as their release from infected macrophages.

The possibility of interfering with either the uPA/uPAR/VN system, RhoA or PKC $\epsilon$  might therefore suggest novel targets to eliminate such an intracellular virion reservoir by facilitating virion release from tissue macrophages, including uPAR<sup>+</sup>/CD68<sup>+</sup> macrophages accumulating virions described in the CNS of HIV<sup>+</sup> individuals [13].

## Supporting Information

### Figure S1 UPA-mediated vesicles formation and accumulation of virions into vesicles are dependent of PKC $\epsilon$ .

U1 cells were preincubated for 45–60 min at 37°C with myristoylated peptides specific for PKC $\epsilon$  isoform and were then stimulated with PMA in the presence or absence of uPA for 48–72 h, then prepared for and analyzed by EM as described in material and methods. Four representative images are shown for each treatment (the third picture of the first panel shows enlargement of virion). Scale bar is reported at the bottom of each picture.

(TIF)

### Figure S2 PKC $\epsilon$ does not influence IL-6 induced HIV expression.

U1 cells were preincubated for 45–60 min at 37°C with myristoylated peptides specific for PKC $\epsilon$  isoform and were then stimulated IL-6, then prepared for and analyzed by EM as described in material and methods. Four representative images are shown for each treatment (the third picture of the first panel shows enlargement of virion). Scale bar is reported at the bottom of each picture. (B) Culture supernatants were analyzed 48 h later for the levels of virus expression (mean  $\pm$  SD of duplicate cultures).

(TIF)

### Figure S3 PMA-induced cell aggregation is prevented by uPA and reversed by blocking small GTPase RhoA and PKC $\delta$ or PKC $\epsilon$ activation.

(A) U1 cells were preincubated for 45–60 min at 37°C with either RhoA23 or RhoA92 Trojan peptides and were then stimulated with PMA in the presence or absence of uPA. Cells were left in their original culture well (not washed to allow persistence of both adherent and suspended cells). Pictures were shot 48 h later for visualizing homotypic cellular clustering (objective magnification 40 $\times$ ). The results of one experiments representative of 4 independently performed are shown. P1; penetratin was used as negative control of Trojan peptides. (B) U1 cells were pre-incubated for 45–60 min at 37°C with myristoylated peptides specific for different PKC isoforms and were then stimulated with PMA in the presence or absence of uPA. Cells were left in the original culture well and pictured 48 h later for homotypic cellular clustering (objective magnification 40 $\times$ ). The results of one experiments representative of 4 independently performed are shown. “Scramble” indicates an irrelevant myristoylated peptide used as negative control.

(TIF)

### Figure S4 uPA induced cell polarization is reversed by blocking RhoA and PKC $\epsilon$ .

A and B. Cells were stimulated as described in Figure 1 and then washed to remove non-adherent cells. Arrowheads indicated polarized structures. Pictures (magnification: 40 $\times$ ) from 1 experiment representative of 11 independently performed are shown.

(TIF)

### Figure S5 Analysis of cell morphology and associated cell width/length ratio.

(A) U1 cells were loaded with cell tracker and then stimulated with PMA+uPA. Adherent cells were stained 2 days later for visualizing their nuclei. Representative cells (objective magnification of 40 $\times$ ) and their form factor are shown. Red dotted shapes are automatically generated by the IN Cell Investigator Software, based of the distribution of cell tracker, and used to calculate the form factor. (B) A total of 1142 and 2245 adherent cells were counted in PMA and PMA+uPA stimulated cells. Unlike what shown in Figure 4B, width/length ratio axis also includes non polarized cells, meaning ratios between 0.8 and 1. Panels C and D represent the absolute percentage of polarized

(ratio below 0.8) and adherent cells and the inter-assay variation between experiments, respectively. (TIF)

**Figure S6 Actin distribution in U1 stimulated cells.** U1 cells were stimulated with PMA in the presence or absence of uPA/CytD and actin distribution in adherent cells was visualized after 48 h of culture by confocal microscopy. Hoechst-33342, DNase I (Alexa Fluor 488, green) and phalloidin (Alexa Fluor 633, red) were used to discriminate nuclei, globular (G actin) and filamentous (F actin) isoforms, respectively. Upper panels show PMA stimulated U1 cells in absence or presence of uPA; bottom panels show CytD stimulated U1 cells in absence or presence of PMA. Image J software was used to perform montage of the three colors. One experiment out of three with similar results is shown. Images were acquired with 63 $\times$  magnification by Leica TCS SP2 confocal microscope. (TIF)

**Figure S7 Different modulation of G and F actin distribution by uPA and CytD in stimulated U1 cells.** U1 cells were stimulated and treated as described in the legend of figure S5. Upper panels show G-actin distribution in U1 cells

cultivated with all different stimuli; bottom panels show F-actin in the same stimulated U1 cells. Images were acquired with 63 $\times$  magnification by Leica TCS SP2 confocal microscope and electronically zoomed 3 times. (TIF)

## Acknowledgments

We are very grateful to Andrew P. Mazar (Chemistry of Life Processes Institute, Evanston, IL) for providing uPA, to Daniele Zacchetti (San Raffaele Scientific Institute, Milan, Italy) for helpful suggestions on experiments of PKC translocation, Maria Carla Panzeri, Miriam Ascagni and Cesare Covino (ALEMBIC, San Raffaele Scientific Institute) for the ultrastructural study, InCell Analyzer analysis and confocal microscopy, respectively, and Alessio Montresor (University of Verona, Verona, Italy) for helpful discussion on the setting of cell polarization assay.

## Author Contributions

Conceived and designed the experiments: CL MA. Performed the experiments: FG CE MA. Analyzed the data: MA. Contributed reagents/materials/analysis tools: CL. Wrote the paper: FG CL GP MA.

## References

- Dano K, Andreasen PA, Grondahl-Hansen J, Kristensen P, Nielsen LS, et al. (1985) Plasminogen activators, tissue degradation, and cancer. *Adv Cancer Res* 44: 139–266.
- Blasi F, Vassalli JD, Dano K (1987) Urokinase-type plasminogen activator: proenzyme, receptor, and inhibitors. *J Cell Biol* 104: 801–804.
- Blasi F, Carmeliet P (2002) uPAR: a versatile signalling orchestrator. *Nat Rev Mol Cell Biol* 3: 932–943.
- Ossowski L, Aguirre-Ghiso JA (2000) Urokinase receptor and integrin partnership: coordination of signaling for cell adhesion, migration and growth. *Curr Opin Cell Biol* 12: 613–620.
- Blasi F (1997) uPA, uPAR, PAI-1: key intersection of proteolytic, adhesive and chemotactic highways? *Immunol Today* 18: 415–417.
- Sidenius N, Siderius N, Blasi F, Poli G (2003) The role of urokinase-type plasminogen activator (uPA)/uPA receptor in HIV-1 infection. *J Leukoc Biol* 74: 750–756.
- Sier CF, Nicoletti I, Santovito ML, Frandsen T, Aletti G, et al. (2004) Metabolism of tumour-derived urokinase receptor and receptor fragments in cancer patients and xenografted mice. *Thromb Haemostasis* 91: 403–411.
- Sidenius N, Sier CF, Ullum H, Pedersen BK, Lepri AC, et al. (2000) Serum level of soluble urokinase-type plasminogen activator receptor is a strong and independent predictor of survival in human immunodeficiency virus infection [In Process Citation]. *Blood* 96: 4091–4095.
- Andersen O, Eugen-Olsen J, Kofoed K, Iversen J, Haugaard SB (2008) Soluble urokinase plasminogen activator receptor is a marker of dysmetabolism in HIV-infected patients receiving highly active antiretroviral therapy. *J Med Virol* 80: 209–216.
- Sidenius N, Sier CF, Ullum H, Pedersen BK, Lepri AC, et al. (2000) Serum level of soluble urokinase-type plasminogen activator receptor is a strong and independent predictor of survival in human immunodeficiency virus infection. *Blood* 96: 4091–4095.
- Ostrowski SR, Katzenstein TL, Pedersen M, Hoyer-Hansen G, Gerstoft J, et al. (2006) Plasma levels of intact and cleaved urokinase receptor decrease in HIV-1-infected patients initiating highly active antiretroviral therapy. *Scand J Immunol* 63: 478–486.
- Sporer B, Koedel U, Popp B, Paul R, Pfister HW (2005) Evaluation of cerebrospinal fluid uPA, PAI-1, and soluble uPAR levels in HIV-infected patients. *J Neuroimmunol* 163: 190–194.
- Cinque P, Nebuloni M, Santovito ML, Price RW, Gisslen M, et al. (2004) The urokinase receptor is overexpressed in the AIDS dementia complex and other neurological manifestations. *Ann Neurol* 55: 687–694.
- Alfano M, Sidenius N, Panzeri B, Blasi F, Poli G (2002) Urokinase-urokinase receptor interaction mediates an inhibitory signal for HIV-1 replication. *Proc Natl Acad Sci U S A* 99: 8862–8867.
- Elia C, Cassol E, Sidenius N, Blasi F, Castagna A, et al. (2007) Inhibition of HIV replication by the plasminogen activator is dependent on vitronectin-mediated cell adhesion. *J Leukoc Biol* 82: 1212–1220.
- Alfano MC, L. Poli G (2006) Glycosyl phosphatidylinositol-anchored proteins and HIV infection. *Letters in Drug Design and Discovery* 3: 598–604.
- Shushakova N, Tkachuk N, Dangers M, Tkachuk S, Park JK, et al. (2005) Urokinase-induced activation of the gp130/Tyk2/Stat3 pathway mediates a pro-inflammatory effect in human mesangial cells via expression of the anaphylatoxin C5a receptor. *J Cell Sci* 118: 2743–2753.
- Simon DI, Rao NK, Xu H, Wei Y, Majdic O, et al. (1996) Mac-1 (CD11b/CD18) and the urokinase receptor (CD87) form a functional unit on monocytic cells. *Blood* 88: 3185–3194.
- Alfano M, Mariani SA, Elia C, Pardi R, Blasi F, et al. (2009) Ligand-engaged urokinase-type plasminogen activator receptor and activation of the CD11b/CD18 integrin inhibit late events of HIV expression in monocytic cells. *Blood* 113: 1699–1709.
- Wada M, Wada NA, Shirono H, Taniguchi K, Tsuchie H, et al. (2001) Amino-terminal fragment of urokinase-type plasminogen activator inhibits HIV-1 replication. *Biochem Biophys Res Commun* 284: 346–351.
- Stevenson M (2003) HIV-1 pathogenesis. *Nat Med* 9: 853–860.
- Gendelman HE, Lipton SA, Tardieu M, Bukrinsky MI, Nottet HS (1994) The neuropathogenesis of HIV-1 infection. *J Leukoc Biol* 56: 389–398.
- Biswas P, Poli G, Kinter AL, Justement JS, Stanley SK, et al. (1992) Interferon gamma induces the expression of human immunodeficiency virus in persistently infected promonocytic cells (U1) and redirects the production of virions to intracytoplasmic vacuoles in phorbol myristate acetate-differentiated U1 cells. *J Exp Med* 176: 739–750.
- Fantuzzi L, Spadaro F, Vallanti G, Canini I, Ramoni C, et al. (2003) Endogenous CCL2 (monocyte chemoattractant protein-1) modulates human immunodeficiency virus type-1 replication and affects cytoskeleton organization in human monocyte-derived macrophages. *Blood*.
- Mulloy JC, Cancelas JA, Filippi MD, Kalfa TA, Guo F, et al. Rho GTPases in hematopoiesis and hemopathies. *Blood* 115: 936–947.
- Alfano M, Rizzi C, Poli G, Biswas P (2007) HIV-1 Infection of promonocytic U937 and U1 cell lines. Clonal distribution of innate restriction factors. In: Herbein G, ed. *HIV and the Macrophage*. Kerala, India: Transworld Research Network, pp 89–113.
- Ploug M, Ellis V (1994) Structure-function relationships in the receptor for urokinase-type plasminogen activator. Comparison to other members of the Ly-6 family and snake venom alpha-neurotoxins. *FEBS Lett* 349: 163–168.
- Konecny G, Untch M, Pihan A, Kimmig R, Gropp M, et al. (2001) Association of urokinase-type plasminogen activator and its inhibitor with disease progression and prognosis in ovarian cancer. *Clin Cancer Res* 7: 1743–1749.
- Sidenius N, Nebuloni M, Sala S, Zerbi P, Price RW, et al. (2004) Expression of the urokinase plasminogen activator and its receptor in HIV-1-associated central nervous system disease. *J Neuroimmunol* 157: 133–139.
- Giagulli C, Scarpini E, Ottoboni L, Narumiya S, Butcher EC, et al. (2004) RhoA and zeta PKC control distinct modalities of LFA-1 activation by chemokines: critical role of LFA-1 affinity triggering in lymphocyte in vivo homing. *Immunity* 20: 25–35.
- Fernie BF, Poli G, Fauci AS (1991) Alpha interferon suppresses virion but not soluble human immunodeficiency virus antigen production in chronically infected T-lymphocytic cells. *J Virol* 65: 3968–3971.
- Bhadriraju K, Yang M, Alom Ruiz S, Pirone D, Tan J, et al. (2007) Activation of ROCK by RhoA is regulated by cell adhesion, shape, and cytoskeletal tension. *Exp Cell Res* 313: 3616–3623.
- Slater SJ, Seiz JL, Stagliano BA, Stubbs CD (2001) Interaction of protein kinase C isozymes with Rho GTPases. *Biochemistry* 40: 4437–4445.
- Laurence J, Sikder SK, Jhaveri S, Salmon JE (1990) Phorbol ester-mediated induction of HIV-1 from a chronically infected promonocyte clone: blockade by

- protein kinase inhibitors and relationship to tat-directed trans-activation. *Biochem Biophys Res Commun* 166: 349–357.
35. Thodeti CK, Albrechtsen R, Grauslund M, Asmar M, Larsson C, et al. (2003) ADAM12/syndecan-4 signaling promotes beta 1 integrin-dependent cell spreading through protein kinase C $\alpha$  and RhoA. *J Biol Chem* 278: 9576–9584.
  36. Mackay HJ, Twelves CJ (2007) Targeting the protein kinase C family: are we there yet? *Nat Rev Cancer* 7: 554–562.
  37. Busso N, Masur SK, Lazega D, Waxman S, Ossowski L (1994) Induction of cell migration by pro-urokinase binding to its receptor: possible mechanism for signal transduction in human epithelial cells. *J Cell Biol* 126: 259–270.
  38. Kamiya K, Ryer E, Sakakibara K, Zohlman A, Kent KC, et al. (2007) Protein kinase C $\delta$  activated adhesion regulates vascular smooth muscle cell migration. *J Surg Res* 141: 91–96.
  39. Kindzelskii AL, Laska ZO, Todd RF, 3rd, Petty HR (1996) Urokinase-type plasminogen activator receptor reversibly dissociates from complement receptor type 3 (alpha M beta 2' CD11b/CD18) during neutrophil polarization. *J Immunol* 156: 297–309.
  40. Estreicher A, Muhlhäuser J, Carpentier JL, Orci L, Vassalli JD (1990) The receptor for urokinase type plasminogen activator polarizes expression of the protease to the leading edge of migrating monocytes and promotes degradation of enzyme inhibitor complexes. *J Cell Biol* 111: 783–792.
  41. Soedel RD, Zeelenberg IS, Gluschankof P (2001) Stromal cell-derived factor-1-induced LFA-1 activation during in vivo migration of T cell hybridoma cells requires Gq/11, RhoA, and myosin, as well as Gi and Cdc42. *J Immunol* 166: 4293–4301.
  42. Larsson C (2006) Protein kinase C and the regulation of the actin cytoskeleton. *Cell Signal* 18: 276–284.
  43. Picone R, Kajaniak EL, Nielsen LS, Behrendt N, Mastronicola MR, et al. (1989) Regulation of urokinase receptors in monocytelike U937 cells by phorbol ester phorbol myristate acetate. *J Cell Biol* 108: 693–702.
  44. Audoly G, Popoff MR, Gluschankof P (2005) Involvement of a small GTP binding protein in HIV-1 release. *Retrovirology* 2: 48.
  45. Sasaki H, Nakamura M, Ohno T, Matsuda Y, Yuda Y, et al. (1995) Myosin-actin interaction plays an important role in human immunodeficiency virus type 1 release from host cells. *Proc Natl Acad Sci U S A* 92: 2026–2030.
  46. Ren XD, Kiosses WB, Schwartz MA (1999) Regulation of the small GTP-binding protein Rho by cell adhesion and the cytoskeleton. *Embo J* 18: 578–585.
  47. Luckenbill-Edds L (1990) Effect of cytochalasin D on the adhesion of a neuroblastoma x glioma cell line (NG108-15) to laminin and plastic substrates. *Cell Tissue Res* 260: 485–493.
  48. Casella JF, Flanagan MD, Lin S (1981) Cytochalasin D inhibits actin polymerization and induces depolymerization of actin filaments formed during platelet shape change. *Nature* 293: 302–305.
  49. Wakatsuki T, Schwab B, Thompson NC, Elson EL (2001) Effects of cytochalasin D and latrunculin B on mechanical properties of cells. *J Cell Sci* 114: 1025–1036.
  50. Kiian I, Tkachuk N, Haller H, Dumler I (2003) Urokinase-induced migration of human vascular smooth muscle cells requires coupling of the small GTPases RhoA and Rac1 to the Tyk2/PI3-K signalling pathway. *Thromb Haemost* 89: 904–914.
  51. Laudanna C, Campbell JJ, Butcher EC (1996) Role of Rho in chemoattractant-activated leukocyte adhesion through integrins. *Science* 271: 981–983.
  52. Bolomini-Vittori M, Montresor A, Giagulli C, Staunton D, Rossi B, et al. (2009) Regulation of conformer-specific activation of the integrin LFA-1 by a chemokine-triggered Rho signaling module. *Nat Immunol* 10: 185–194.
  53. Surin B, Rouillard D, Bauvois B (2002) Interactions between human monocytes and fibronectin are suppressed by interferons beta and gamma, but not alpha: correlation with Rho-paxillin signaling. *Int J Mol Med* 10: 25–31.
  54. Aepfelbacher M, Essler M, Huber E, Czech A, Weber PC (1996) Rho is a negative regulator of human monocyte spreading. *J Immunol* 157: 5070–5075.
  55. Cavnar PJ, Berthier E, Beebe DJ, Huttenlocher A. Hax1 regulates neutrophil adhesion and motility through RhoA. *J Cell Biol* 193: 465–473.
  56. Wang L, Zhang H, Solski PA, Hart MJ, Der CJ, et al. (2000) Modulation of HIV-1 replication by a novel RhoA effector activity. *J Immunol* 164: 5369–5374.
  57. Hodges A, Sharrocks K, Edelmann M, Baban D, Moris A, et al. (2007) Activation of the lectin DC-SIGN induces an immature dendritic cell phenotype triggering Rho-GTPase activity required for HIV-1 replication. *Nat Immunol* 8: 569–577.
  58. Fackler OT, Krausslich HG (2006) Interactions of human retroviruses with the host cell cytoskeleton. *Curr Opin Microbiol* 9: 409–415.
  59. Ott DE, Coren LV, Johnson DG, Kane BP, Sowder RC, 2nd, et al. (2000) Actin-binding cellular proteins inside human immunodeficiency virus type 1. *Virology* 266: 42–51.
  60. Kinter AL, Poli G, Maury W, Folks TM, Fauci AS (1990) Direct and cytokine-mediated activation of protein kinase C induces human immunodeficiency virus expression in chronically infected promonocytic cells. *J Virol* 64: 4306–4312.
  61. Rabbi MF, al-Harhi L, Saifuddin M, Roebuck KA (1998) The cAMP-dependent protein kinase A and protein kinase C-beta pathways synergistically interact to activate HIV-1 transcription in latently infected cells of monocyte/macrophage lineage. *Virology* 245: 257–269.
  62. Wolf D, Giese SI, Witte V, Krautkramer E, Trapp S, et al. (2008) Novel (n)PKC kinases phosphorylate Nef for increased HIV transcription, replication and perinuclear targeting. *Virology* 370: 45–54.
  63. Ivaska J, Vuoriluoto K, Huovinen T, Izawa I, Inagaki M, et al. (2005) PKC $\epsilon$ -mediated phosphorylation of vimentin controls integrin recycling and motility. *Embo J* 24: 3834–3845.
  64. Wichroski MJ, Ichiyama K, Rana TM (2005) Analysis of HIV-1 viral infectivity factor-mediated proteasome-dependent depletion of APOBEC3G: correlating function and subcellular localization. *J Biol Chem* 280: 8387–8396.
  65. Karczewski MK, Strebel K (1996) Cytoskeleton association and virion incorporation of the human immunodeficiency virus type 1 Vif protein. *J Virol* 70: 494–507.
  66. Shoeman RL, Huttermann C, Hartig R, Traub P (2001) Amino-terminal polypeptides of vimentin are responsible for the changes in nuclear architecture associated with human immunodeficiency virus type 1 protease activity in tissue culture cells. *Mol Biol Cell* 12: 143–154.
  67. Vieira OV, Botelho RJ, Grinstein S (2002) Phagosome maturation: aging gracefully. *Biochem J* 366: 689–704.
  68. Carter CA, Ehrlich LS (2008) Cell biology of HIV-1 infection of macrophages. *Annu Rev Microbiol* 62: 425–443.
  69. Banerjee J, Wedegaertner PB (2004) Identification of a novel sequence in PDZ-RhoGEF that mediates interaction with the actin cytoskeleton. *Mol Biol Cell* 15: 1760–1775.
  70. Niggli V (2003) Microtubule-disruption-induced and chemotactic-peptide-induced migration of human neutrophils: implications for differential sets of signalling pathways. *J Cell Sci* 116: 813–822.
  71. Laudanna C, Alon R (2006) Right on the spot. Chemokine triggering of integrin-mediated arrest of rolling leukocytes. *Thromb Haemost* 95: 5–11.
  72. Azab AK, Azab F, Blotta S, Pitsillides CM, Thompson B, et al. (2009) RhoA and Rac1 GTPases play major and differential roles in stromal cell-derived factor-1-induced cell adhesion and chemotaxis in multiple myeloma. *Blood* 114: 619–629.
  73. Faix J, Breitsprecher D, Stradal TE, Rottner K (2009) Filopodia: Complex models for simple rods. *Int J Biochem Cell Biol* 41: 1656–1664.
  74. Madsen CD, Sarra Ferraris GM, Andolfo AP, Cunningham O, Sidenius N (2007) uPAR-induced cell adhesion and migration: vitronectin provides the key. *Journal of Cell Biology* 177: 927–939.
  75. Sidenius N, Andolfo A, Fesce R, Blasi F (2002) Urokinase regulates vitronectin binding by controlling urokinase receptor oligomerization. *J Biol Chem* 277: 27982–27990.
  76. Madsen CD, Sidenius N (2008) The interaction between urokinase receptor and vitronectin in cell adhesion and signalling. *Eur J Cell Biol* 87: 617–629.
  77. Petzinger J, Saltel F, Hersemeyer K, Daniel JM, Preissner KT, et al. (2007) Urokinase receptor (CD87) clustering in detergent-insoluble adhesion patches leads to cell adhesion independently of integrins. *Cell Commun Adhes* 14: 137–155.
  78. Ridley AJ, Schwartz MA, Burridge K, Firtel RA, Ginsberg MH, et al. (2003) Cell migration: integrating signals from front to back. *Science* 302: 1704–1709.